Influence of Separated Wing Flow on Tail Downwash of Low-Wing Pusher Configuration

K. Karthik,* E. G. Tulapurkara,† and K. A. Damodaran‡
Indian Institute of Technology, Madras, Chennai 600 036, India

Introduction

A REVIEW of the various types of airplanes currently in use as ab-initio trainers (e.g., *Jane's All the World's Aircraft*, 1988–89) reveals that these designs predominantly feature a tractor (front-engined) configuration with a conventional wing and tail arrangement. However, unconventional configurations with a pod-and-boom fuselage and a pusher engine offer advantages such as reduced drag, improved visibility for the pilots, and lower noise levels. These advantages have been studied by Strojnik[1] and Carmichael.[2] Based on similar considerations, Sharma[3] had proposed a pusher-engined, pod-and-boom design for a two-seat ab-initio trainer.

Wind-tunnel tests on a model of this airplane showed,[4] as compared to theoretical estimates, much lower lift curve slope, much higher induced drag, and much higher static stability. The tests also indicated a significant region of separated flow near the wing root. Taking clues from this and observations made by Muttray,[5] the lift distribution on the wing was calculated, in the present investigation, with regions of separated flow nearly equal to those indicated by flow visualization. In this region the local lift-curve slope is assigned a very small value. Calculated lift-curve slope of wing, induced drag, and downwash closely match the experimental values and serve to explain the unusual behavior of the configuration. The configuration and results of wind-tunnel tests are briefly described in the next section. Calculation of the lift distribution with a region of separated flow and results and discussion are presented subsequently.

Configuration and Test Results

The configuration of the low-wing pod-and-boom airplane with a pusher engine is shown in Fig. 1. Important dimensions are also given. Ashok et al.[6] give a detailed description of the configuration. Karthik[7] has estimated the characteristics of the airplane using methods described by Smetana et al.[8] and U.S. Air Force DATCOM. Lift coefficient C_L vs angle of attack α, drag coefficient C_D vs C_L^2, and moment coefficient C_m vs C_L are shown in Fig. 2. The wind-tunnel tests[4] were conducted on a one-seventh scale model in the 4.2 × 3 m wind tunnel of the Indian Institute of Science, Bangalore, India. The Reynolds number, based on the aerodynamic chord of the model wing (0.178 m) and the freestream velocity (40 m/s), was 0.4×10^6. The model was tested without the propeller. The flow over the model was tripped by the use of grits, which were located at 10% local chord on the wing and tail surfaces and at 10% of body length for the fuselage. Two grits with broad (10 mm wide) and narrow (5 mm wide) were used. The C_m vs C_L curve and the minimum drag coefficient were almost the same for the two grits, indicating that the boundary layers were fully tripped in both cases. The angle of attack α was varied between $-10°$ to $16°$ in steps of $2°$. The experimental results are shown in Fig. 2. The value of the Oswald efficient factor e from experimental data is 0.3, whereas the estimated value is 0.88. Further, the value of downwash gradient $d\varepsilon/d\alpha$ deduced from experiments is roughly -0.46, whereas estimates indicate a positive value of 0.37. This upwash over the horizontal tail was, at first sight, unexpected.

Received 19 March 1998; revision received 15 May 1999; accepted for publication 19 May 1999.

*Research Scholar, Department of Aerospace Engineering.

†Professor, Department of Aerospace Engineering. Associate Fellow AIAA.

‡Professor, Department of Aerospace Engineering.

Span	= 11·81 m	Max. fuselage height	= 1·01 m
Length	= 5·97 m	Max. fuselage width	= 1·16 m
Height	= 2·24 m	Horizontal tail area	= 2·22 m^2
Wing area	= 13·91 m^2	Horizontal tail span	= 3·70 m
Wing aspect ratio	= 10·03	Tail volume ratio	= 0·471
Fuselage (pod) length	= 2·78 m		

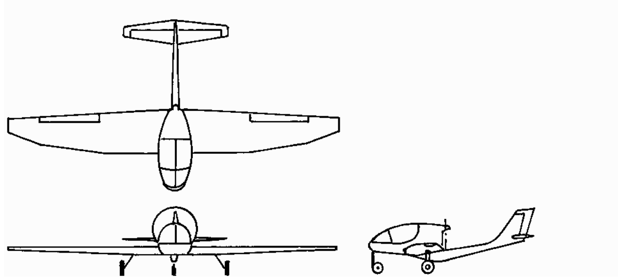

Fig. 1 Airplane configuration.

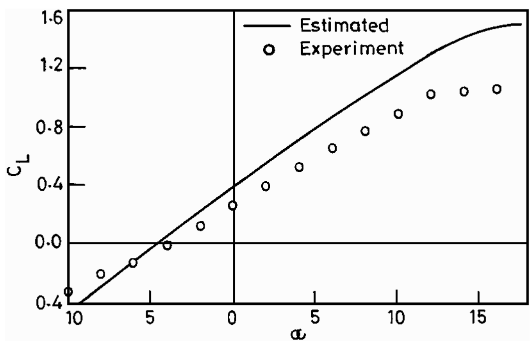

C_L vs α

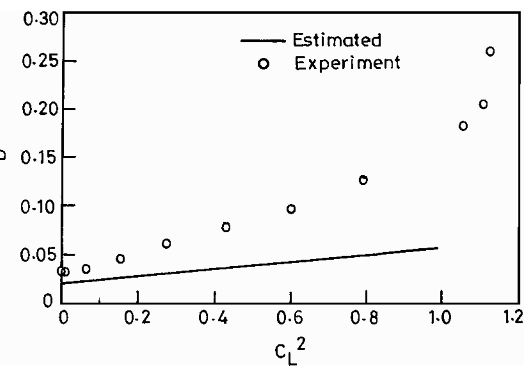

C_D vs C_L^2

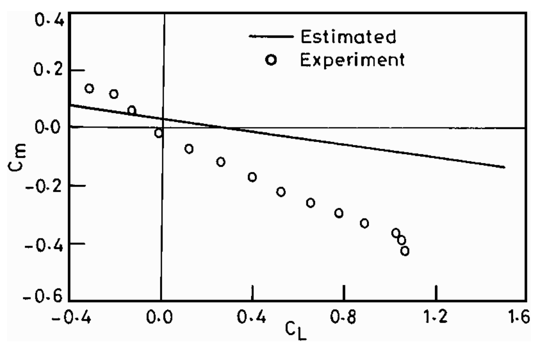

C_m vs C_L

Fig. 2 Airplane characteristics.

Flow visualization studies were also carried out,[7] which indicated that there was flow separation near the wing root over the entire wing chord at all angles of attack. It is surmised[4] that the separation on the wing at all angles of attack is caused by the fact that both fuselage and the wing terminate at the same streamwise station. The separated region extended between 25 to 28% of wing as shown in Fig. 3. From this the conclusion was made that the inboard portion of the wing extending to about 25% of the span is producing only negligible

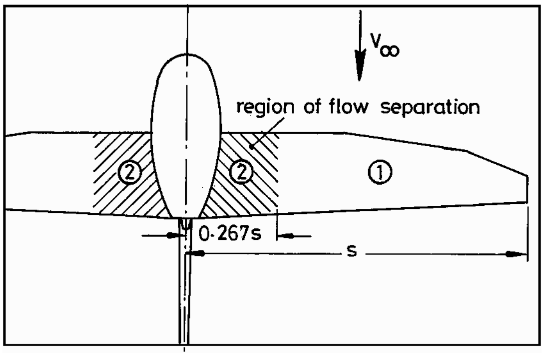

Fig. 3 Observed spanwise extent of separated flow.

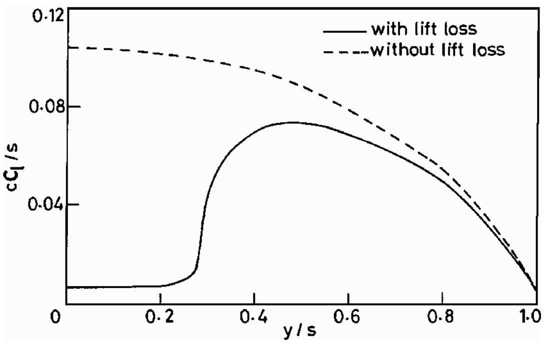

Fig. 4 Spanwise load distribution.

lift. Hoerner and Borst[9] have quoted results of Muttray,[5] wherein experimental investigation on wing with trailing-edge cutouts near wing root showed that some portion of the tail experienced upwash. These two viz. flow visualization results and Muttray's findings led to the inference that loss of lift near the root could result in upwash at the tail. However, downwash/upwash at the tail can be calculated, fairly accurately, once the lift distribution on the wing is known. In the present investigation downwash calculations have been done with negligible lift near the wing root. Details are summarized in the next section.

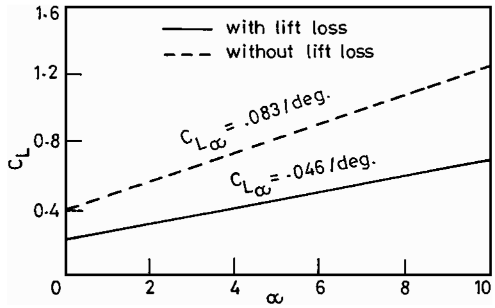

C_L vs α

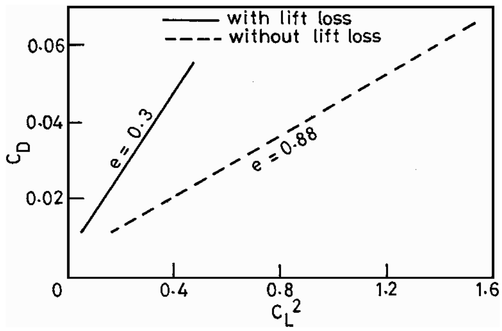

C_D vs C_L^2

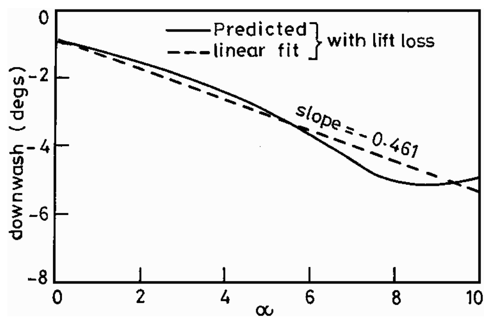

Mean downwash vs α

Fig. 5 Characteristics with and without lift loss.

Numerical Study and Results

To study the effects of flow separation on spanwise distribution of lift, induced drag, and downwash, a numerical study was undertaken. It utilizes the lifting-line theory described by McCormick[10] and the downwash estimation method of Silverstein et al.[11] that accounts for the downward displacement of the vortex sheet. The implimentation details are given in Karthik.[7]

The numerical computation has been carried out using 30 control points along the span. Trials with a different number of control points indicated that spanwise load distribution converged with more than 20 grid points. To take into account the lift loss, the assumption was made that the slope of the lift curve $C_{1\alpha}$ in the region from the root to a certain distance along the span is very small. A value of 0.005 per degree was prescribed. The results are not very sensitive to the value as long as it is small. Elsewhere $C_{1\alpha}$ was prescribed as 0.1 per degree. Lift-curve slope of the wing, induced drag, and downwash at the tail were calculated for different extents of the region where $C_{1\alpha}$ is 0.005 per degree. When the extent was equal to 0.267 of semispan, the calculated values of $C_{L\alpha}$, e, and $\mathrm{d}\varepsilon/\mathrm{d}\alpha$ almost matched with experimental ones. The flow visualization studies indicated that the separation region lies between 25 and 28% of semispan. The spanwise load distributions (cc_1/s vs y/s) with and without lift loss are shown in Fig. 4. C_L vs α curve and C_D vs C_L^2 curves are shown in Fig. 5. The calculated value of average $\mathrm{d}\varepsilon/\mathrm{d}\alpha$ is 0.461, which matches the experimental value. The results confirm that the unusual behavior of the configuration was caused by the effect of lift loss near the root.

Concluding Remarks

A low-wing pod-and-boom combination was found to suffer from almost total loss of lift in the region near the root of the wing. The separated region is almost equal to the tail span. The region of the wing that produces the lift causes an upwash on the tail and results in large static stability, low lift-curve slope, and high induced drag. The results are confirmed by a numerical study that employs a lifting-line theory with a small value of local lift-curve slope in the region of separated flow. Thus a low-wing configuration does not appear to be suitable in combination with pod-and-boom configuration. However, it may be added that, though sandpaper was used to trip the flow, the size of model is rather small and a test at higher Reynolds number may be needed, and the effect of pusher propeller was not simulated in tests. Inflow from a pusher propeller is likely to reduce extent of flow seperation.

References

[1] Strojnik, A., *Low Power Laminar Aircraft Design*, Published by author, Tempe, AZ, 1984.

[2] Carmichael, B. H., "Application of Sailplane and Low-Drag Underwater Vehicle Technology to the Long-Endurance, Drone Problem," *Proceedings of the Second International Symposium on the Technology and Science of Low-Speed and Motorless Flight*, Soaring Society of America, Los Angeles, 1974.

[3] Sharma, N., "Design of a Composite Light Aircraft," M. Tech. Thesis, Department of Aerospace Engineering, Indian Inst. of Technology, Kanpur, 1989.

[4]Narayana Rao, C. K., and Krishnamurthy, M., "Wind Tunnel Test Studies on 1/7 Scale NALLA-1 Model," National Aeronautical Lab., NAL PD EA 9203, Bangalore, India, March 1992.

[5]Muttray, H., "Investigations on the Downwash Behind a Tapered Wing with Fuselage and Propeller," NACA TM 876, 1939.

[6]Ashok, G., Karthik, K., Satish, B. G., and Rohidekar, S. R., "NALLA-1 Data Report," National Aeronautical Lab., NAL PD FE 9102, Bangalore, India, Sept. 1991.

[7]Karthik, K., "Evaluation of a Low-Wing Pod-and-Boom Configuration for a Light Airplane," M.S. Thesis, Indian Inst. of Technology, Madras, Oct. 1992.

[8]Smetana, F. O., Summey, D. C., and Johnson, W. D., "Riding and Handling Qualities of Light Aircraft—A Review and Analysis," NASA CR 1975, March 1972.

[9]Hoerner, S. F., and Borst, H. V., *Fluid Dynamic Lift*, Hoerner Fluid Dynamics, Brick Town, NJ, 1975, pp. 11–19.

[10]McCormick, B. W., *Aerodynamics, Aeronautics and Flight Mechanics*, Wiley, New York, 1979, pp. 187–193.

[11]Silverstein, A., Katzoff, S., and Bullivant, W. K., "Downwash and Wake Behind Plain and Flapped Airfoils," NACA TR 651, 1939.